Differentiation of Intramedullary Neoplasms and Cysts by MR

Alan L. Williams, Victor M. Haughton, Kathleen W. Pojunas, David L. Daniels and David P. Kilgore

AJNR Am J Neuroradiol 1987, 8 (3) 527-532
http://www.ajnr.org/content/8/3/527

Differentiation of Intramedullary Neoplasms and Cysts by MR

Alan L. Williams[1]
Victor M. Haughton
Kathleen W. Pojunas
David L. Daniels
David P. Kilgore

To determine the MR criteria that are effective for differentiating intramedullary neoplasms from syringo- or hydromyelia, we reviewed MR scans made on prototype and commercial imagers of 33 patients with surgically confirmed cord abnormalities, including nine intramedullary neoplasms and 20 cysts (syringo- or hydromyelia). Two radiologists who did not know the clinical and radiologic diagnoses were asked to evaluate the scans with respect to (1) cord expansion, (2) distinctness of the disease margin, (3) homogeneity, and (4) signal intensity. These observations were correlated with the proved diagnoses. The combination of distinct margins and uniform signal intensity equal to that of CSF correlated consistently (88%) with spinal cord cysts. Other combinations were less reliable for diagnosing a cyst or tumor.

MR imaging has been shown to demonstrate, effectively and noninvasively, a variety of spinal diseases [1–14]. However, previously described MR criteria for differentiating intramedullary neoplasms and cysts have not been evaluated objectively. Therefore, for the purpose of selecting the most accurate MR criteria, we reviewed a series of patients with surgically confirmed intramedullary abnormalities.

Materials and Methods

MR scans were reviewed in 33 patients (14 males and 19 females ranging in age from 6 to 71 years) with intramedullary lesions studied between May 1983 and November 1985. Scans were acquired on various prototype (0.5–1.5 T) MR imagers at the General Electric facility in New Berlin, WI, or on a 1.5-T commercial MR scanner (GE Signa) at the Milwaukee County Medical Complex. All patients were studied with short TR spin-echo pulse sequences (TR = 500–800 msec,TE = 20–25 msec) and 16 were also studied with long TR spin-echo pulse sequences (TR = 2000–2500 msec,TE = 20–25 msec and 80–100 msec). Scans were obtained with a standard body coil in 16 patients and with 7.5- or 10-cm "butterfly" surface coils (Medical Advances, Inc., Milwaukee, WI) in 17 patients [15]. Other imaging parameters included 3–10 mm slice thickness, 0–2 mm slice interspacing, 2–4 excitations, 4–10 min acquisition time, 128 × 256 or 256 × 256 matrixes, and 16–25 cm field of view. Imaging was routinely performed in the sagittal plane; additional images in the axial plane were obtained in seven patients.

MR scans in the 33 patients were evaluated by two senior radiology residents who did not know the clinical and radiologic diagnoses. The readers were asked to report four different MR observations: (1) expanded cord (larger anteroposterior diameter than the remainder of the cord), (2) distinct or indistinct margins in the disease, (3) uniform or nonuniform signal intensity in the disease, and (4) signal intensity of the disease isointense with CSF or not.

Results

The intramedullary abnormalities included nine neoplasms (five astrocytomas, three ependymomas, and one lipoma), 20 cysts (syrinx or hydromyelia), two cases of myelomalacia, one case of viral myelitis, and one case of hematoma. Diagnoses

This article appears in the May/June 1987 issue of *AJNR* and the July 1987 issue of *AJR*.

Received June 6, 1986; accepted after revision November 21, 1986.

Presented at the annual meeting of the American Society of Neuroradiology, San Diego, January 1986.

[1] All authors: Department of Radiology, Medical College of Wisconsin, Froedtert Memorial Lutheran Hospital, 9200 West Wisconsin Ave., Milwaukee, WI 53226. Address reprint requests to A. L. Williams.

***AJNR* 8:527–532, May/June 1987**
0195–6108/87/0803–0527

were verified at surgery by biopsy, cyst puncture, or, in cases of myelomalacia, intraoperative sonography.

The data are tabulated in two ways: the percentage of cysts or tumors with the MR observation is recorded in Table 1, and the percentage of MR observations in which a cyst was found is recorded in Table 2. In the cases of intramedullary cyst, an expanded cord was reported in 78% of patients, distinct margins in 73%, uniform signal intensity in

TABLE 1: Frequency* (%) of MR Observations in 33 Spinal Cord Lesions

Nosologic Diagnosis	Observation			
	Expanded Cord	Distinct Margins	Uniform Signal Intensity	Isointensity
Neoplasm	78	44	44	17
Syringohydromyelia	78	73	75	78
Other**	38	50	25	38

* Frequency = percentage of the nosologic category with the MR finding.
** Includes myelomalacia, viral myelitis, and hematoma.

TABLE 2: Accuracy* of MR Findings in Predicting a Diagnosis

MR Observation	Nosologic Diagnosis	Diagnostic Accuracy (%)
Distinct margins	Syringohydromyelia	78
Uniform signal intensity	Syringohydromyelia	76
Isointensity (CSF)	Syringohydromyelia	85

* Accuracy = percentage of cases with the MR finding that had the specific nosologic diagnosis.

TABLE 3: Accuracy of MR Findings in Predicting a Diagnosis

MR Observation	Nosologic Diagnosis	Diagnostic Accuracy (%)
Distinct margins, uniform signal intensity, and isointensity (CSF)	Syringohydromyelia	88
Indistinct margins, nonuniform signal intensity, and nonisointensity (CSF)	Neoplasm	60

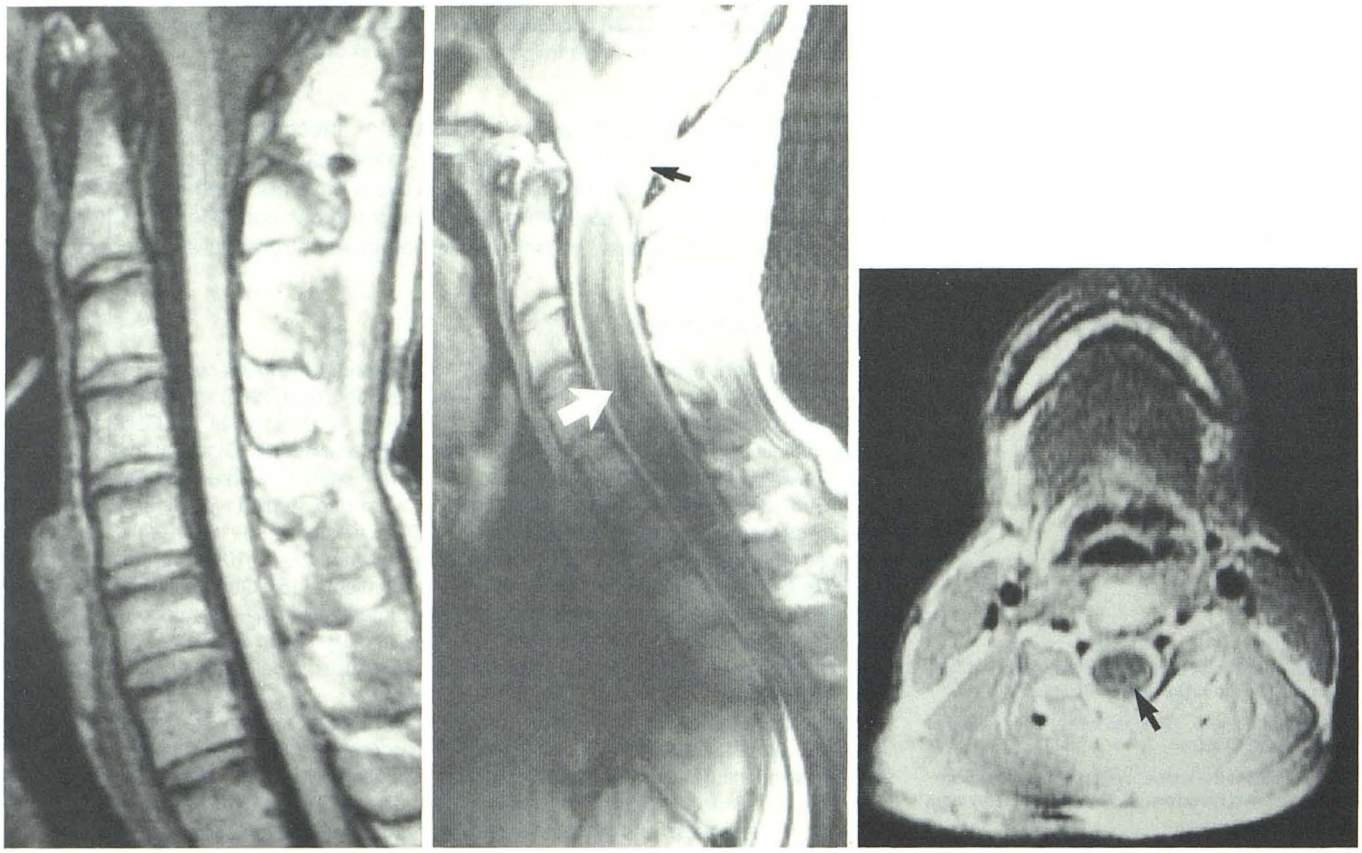

A B

Fig. 1.—Normal cervical cord. In sagittal T1-weighted spin-echo image (TR = 800 msec, TE = 25 msec), cervical spinal cord has virtually uniform anteroposterior dimension and homogeneous signal intensity.

Fig. 2.—Typical MR appearance of hydromyelia in 19-year-old man. Sagittal (*A*) and axial (*B*) short TR spin-echo images (TR = 400 msec, TE = 25 msec) demonstrate marked expansion of cervical central canal (*large arrow*). Cyst margins are well defined and cyst fluid is homogeneous and isointense with CSF. Note low-lying cerebellar tonsils (*small arrow*) in this patient with Chiari I malformation.

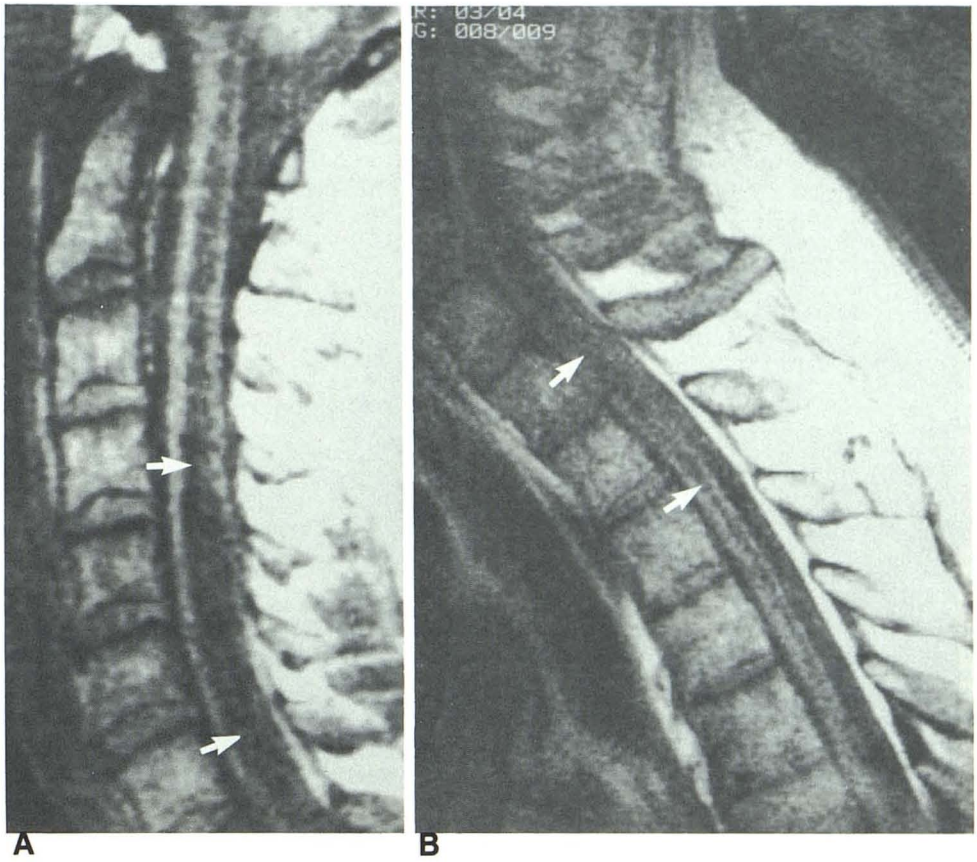

Fig. 3.—Characteristic MR findings in syringomyelia. Sagittal short TR spin-echo images (TR = 600 msec, TE = 25 msec) through cervical (*A*) and cervicothoracic (*B*) regions in 38-year-old man show expansion of mid and lower cervical cord secondary to extensive syrinx (*arrows*). Syrinx margins are well defined and cyst fluid is isointense with CSF.

75%, and isointensity with CSF in 78%. In patients with neoplasm, cord expansion was also reported in 78% of patients, distinct margins in 44%, uniform signal intensity in 44%, and isointensity in 17%. A cyst was confirmed surgically in 78% of reported distinct margins, in 76% of reported uniform signal intensities, and in 85% of reported signal isointensity. When the three criteria—distinct margins, uniform signal intensity, and isointensity—were observed in the same patient, the likelihood of syringo- or hydromyelia was 88% (Table 3). With a combination of indistinct margins, nonuniform signal intensity, and nonisointensity the likelihood of neoplasms was only 60%.

Discussion

Syringomyelia refers to a glial-lined cavity within the spinal cord. Hydromyelia represents cystic dilatation of the cord's central canal. Syringohydromyelia, a nonspecific term describing a nonneoplastic intramedullary cyst, encompasses both syringomyelic and hydromyelic abnormalities.

Conventional CT or myelographic imaging is imperfect in distinguishing intramedullary neoplasm and syringo- or hydromyelia. Myelography does not reliably differentiate intramedullary tumor from cyst because both abnormalities typically show a fusiformly expanded cord as a filling defect within the subarachnoid contrast column [16]. Unenhanced CT may show the cord [17]; however, artifacts from adjacent osseous structures or body parts outside the reconstruction circle tend to obscure the cord margins and small intramedullary cysts. Intrathecally enhanced CT effectively shows cord margins and may demonstrate opacification of intramedullary cysts on immediate or delayed CT scans [18–20]. However, not all cases of syringo- or hydromyelia show intramedullary contrast enhancement, and cystic neoplasms and myelomalacia may also show enhancement within cord substance [21, 22].

The sensitivity of MR for detecting spinal disease is high. Because of its excellent contrast resolution, MR effectively demonstrates the spinal cord (Fig. 1) and detects various intramedullary abnormalities, including syringo- or hydromyelia (Figs. 2 and 3), neoplasm (Figs. 4–7), myelomalacia (Fig. 8), hematoma (Fig. 9), and arteriovenous malformation.

The typical intramedullary cyst is characterized by a glial cell (syringomyelia) or ependymal (hydromyelia) lining, which provides a sharp interface with the cyst fluid. Thus, most cysts appear in MR images as an abnormality with sharply defined margins, uniform signal intensity, and isointensity with CSF (Figs. 2 and 3). Occasionally, collagenous bands or synechiae crossing the cyst cavity from one wall to the other or a high protein concentration in the cyst fluid may produce nonuniform signal intensity, hyperintensity, or ill-defined mar-

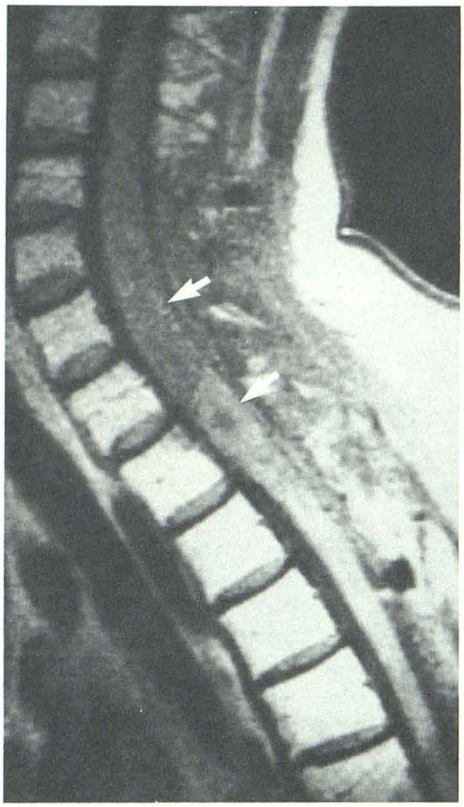

Fig. 4.—Characteristic MR findings in astrocytoma. Short TR spin-echo image (TR = 800 msec, TE = 25 msec) in 53-year-old-woman shows lower cervical cord expanded by inhomogeneous, poorly marginated, intramedullary neoplasm (*arrows*). Signal intensity of tumor is greater than that of CSF.

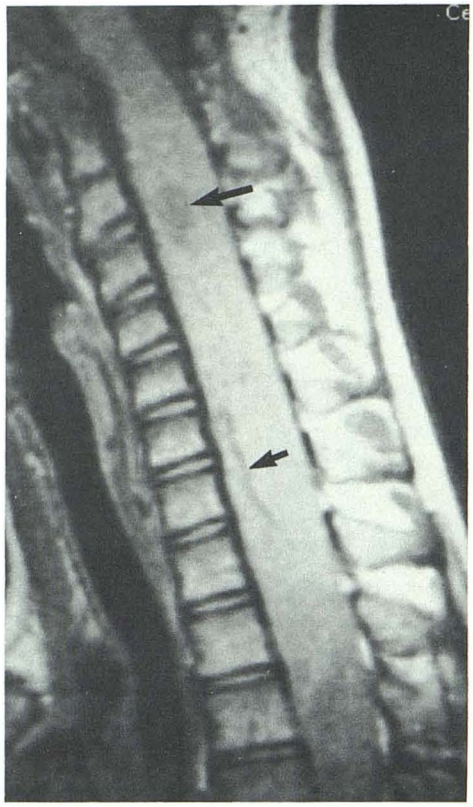

Fig. 5.—Indistinct margins in an ependymoma in 6-year-old boy with neurofibromatosis. Sagittal T1-weighted spin-echo image (TR = 600 msec, TE = 25 msec) shows diffuse expansion of cervical and upper thoracic cord. Tumor margins cannot be distinguished. Note area of cystic degeneration (*large arrow*) and dilated vessel (*small arrow*).

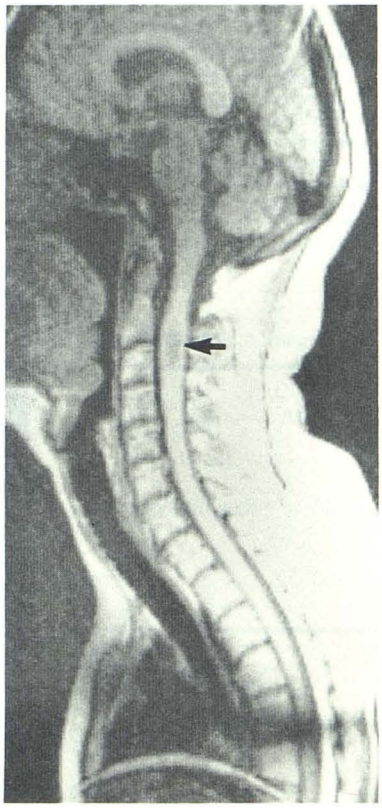

Fig. 6.—Cervical ependymoma. Focal expansion of cord in 43-year-old woman secondary to indistinctly marginated tumor (*arrow*) is identified in T1-weighted spin-echo image (TR = 350 msec, TE = 20 msec). Signal intensity of tumor is intermediate between normal cord and CSF.

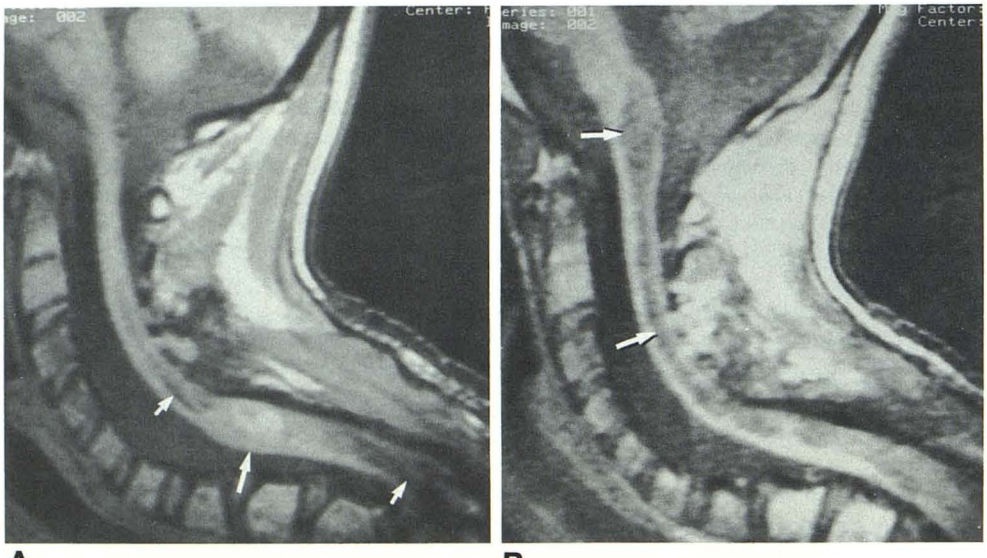

A B

Fig. 7.—*A* and *B*, Astrocytoma with syrinx in 13-year-old boy. Short TR sagittal spin-echo images (TR = 600 msec, TE = 25 msec) show inhomogeneous, hyperintense expansile process (*large arrow* in *A*) at cervicothoracic junction associated with extensive, sharply marginated cervicomedullary and upper thoracic cyst (*small arrows* in *A* and *B*). Patient has had previous surgery and radiation therapy.

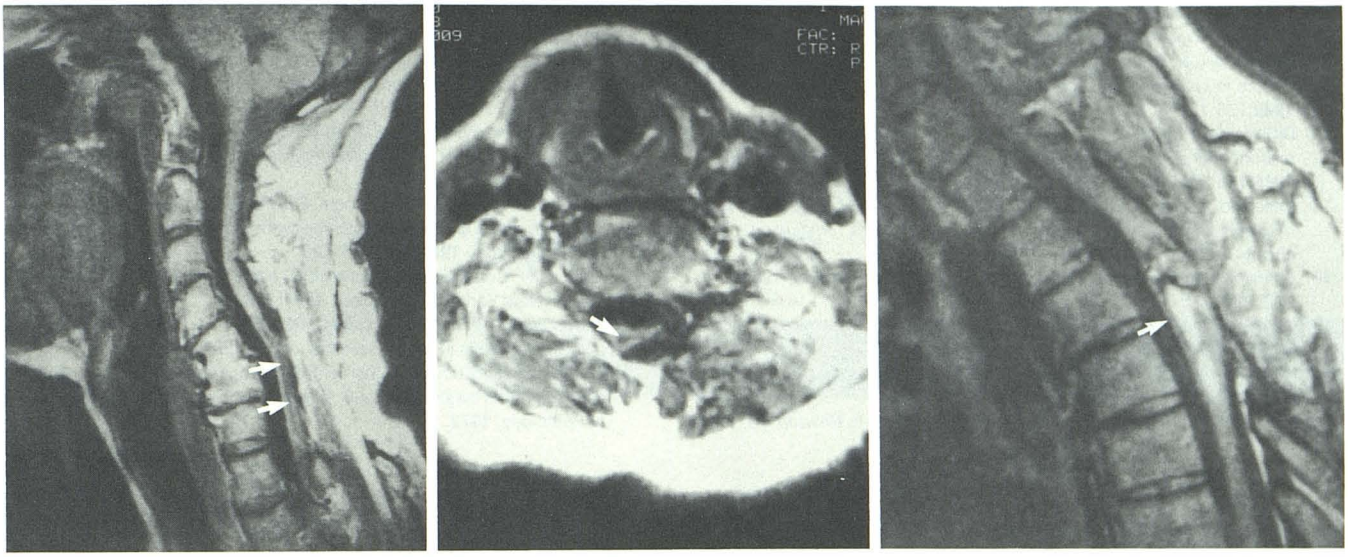

Fig. 8.—Myelomalacia in 53-year-old woman with a history of chronic posttraumatic myelopathy. Sagittal (*A*) and axial (*B*) T1-weighted spin-echo images (TR = 600 msec, TE = 25 msec) show an atrophic, misshapen, lower cervical cord associated with intramedullary zone of decreased signal intensity (*arrows*). Myelomalacia was confirmed by intraoperative sonography. Note solid C5–C6 anterior vertebral fusion and abnormal spinal curvature.

Fig. 9.—Intramedullary hematoma in 30-year-old woman with a history of previous spontaneous intramedullary hemorrhage. Recurrent symptoms prompted MR examination. Sagittal short TR spin-echo image (TR = 800 msec, TE = 25 msec) shows focal expansion of cervicothoracic cord secondary to inhomogeneous process (*arrow*) containing both high and low signal intensity tissue that represents subacute hematoma.

gins [23]. In addition, pulsatile CSF movement may occasionally cause inhomogeneous signal intensity within an intramedullary cyst in T2-weighted images [24]. However, our study suggests that when a combination of three criteria—distinct margins, uniform signal intensity, and isointensity (with CSF)—are observed in MR scans in a patient with an expanded cord, the diagnosis of syringo- or hydromyelia can be made with a high degree of accuracy. In these cases additional imaging studies may not be needed. As surface coil advances and other technical improvements increase MR resolution, even greater accuracy should be noted.

MR is less accurate in characterizing intramedullary tumors. Primary tumors such as astrocytomas and ependymomas tend to infiltrate adjacent cord tissue and evoke reactive edema [25]. This combination of infiltrating tumor and edema results in ill-defined margins in MR images (Figs. 4–6). Necrosis, cystic degeneration, or hemorrhage may cause tumors to have an inhomogeneous MR appearance (Figs. 4, 5, 7). Highly proteinaceous fluid within zones of cystic degeneration may produce hyperintensity or nonuniform signal intensity on MR. Thus, poorly defined margins, inhomogeneity, and lack of isointensity suggest neoplasm. The combination of indistinct margins, nonuniform signal intensity, and nonisointensity was present in a small majority of our tumors but cannot be considered diagnostic of neoplasm. In cases where an intramedullary neoplasm is associated with a syrinx, MR may show features of both abnormalities (Fig. 7).

REFERENCES

1. Norman D, Mills CM, Brant-Zawadzki M, Yeates A, Crooks LE, Kaufman L. Magnetic resonance imaging of the spinal cord and canal: potentials and limitations. *AJR* **1983**;141:1147–1152, *AJNR* **1984**;5:9–14
2. Moon KL, Genant HK, Helms CA, Chafetz NI, Crooks LE, Kaufman L. Musculoskeletal applications of nuclear magnetic resonance. *Radiology* **1983**;147:161–171
3. Han JS, Kaufman B, El Yousef SJ, et al. NMR imaging of the spine. *AJNR* **1983**;4:1151–1159
4. Modic MT, Weinstein MA, Pavlicek W, et al. Nuclear magnetic resonance imaging of the spine. *Radiology* **1983**;148:757–762
5. Modic MT, Weinstein MA, Pavlicek W, Boumphrey F, Starnes D, Duchesneau PM. Magnetic resonance imaging of the cervical spine: technical and clinical observations. *AJNR* **1984**;5:15–22
6. Bradley WG, Waluch V, Yadley RA, Wycoff RR. Comparison of CT and MR in 400 patients with suspected disease of the brain and cervical spinal cord. *Radiology* **1984**;152:695–702
7. Pojunas K. Williams AL, Daniels DL, Haughton VM. Syringomyelia and hydromyelia: magnetic resonance evaluation. *Radiology* **1984**;153:679–683
8. Gebarski SS, Maynard FW, Gabrielsen TO, Knake JE, Latack JT, Hoff JT. Posttraumatic progressive myelopathy. Clinical and radiologic correlation employing MR imaging, delayed CT metrizamide myelography and intraoperative sonography. *Radiology* **1985**;157:379–385
9. Spinos E, Laster DW, Moody DM, Ball MR, Witcofski RL, Kelly DL. MR evaluation of Chiari I malformations at 0.15 T. *AJNR* **1985**;6:203–208
10. Hyman RA, Edwards JH, Vacirca SJ, Stein HL. 0.6 T MR imaging of the cervical spine: multislice and multi-echo techniques. *AJNR* **1985**;6:229–236
11. Lee BCP, Zimmerman RD, Manning JJ, Deck MDF. MR imaging of syringomyelia and hydromyelia. *AJNR* **1985**;6:221–228

12. Baker HL, Berquist TH, Kispert DB, et al. Magnetic resonance imaging in a routine clinical setting. *Mayo Clin Proc* **1985**;60:75–90
13. Kucharczyk W, Brant-Zawadzki M, Sobel D, et al. Central nervous system tumors in children: detection by magnetic resonance imaging. *Radiology* **1985**;155:131–136
14. DiChiro G, Doppman JL, Dwyer AJ, et al. Tumors and arteriovenous malformations of the spinal cord: assessment using MR. *Radiology* **1985**;156:689–697
15. Kneeland JB, Jesmanowicz A, Froncisz W, Grist TM, Hyde JS. High-resolution MR imaging using loop-gap resonators. *Radiology* **1986**; 158:247–250
16. Shapiro R: *Myelography*, 4th ed. Chicago: Year Book Medical, **1984**:218–222, 346–358
17. Haughton VM, Williams AL. *Computed tomography of the spine.* St. Louis: Mosby, **1982**:31–41
18. Aubin ML, Vignaud J, Jardin C, Bar D. Computed tomography in 75 clinical cases of syringomyelia. *AJNR* **1981**;2:199–204
19. Dorwart RH, LaMasters DL, Watanabe TJ. Tumors. In Newton TH, Potts DG, eds. *Computed tomography of the spine and spinal cord: modern neuroradiology*, vol. 1. San Anselmo, CA: Clavadel Press, **1983**:115–147
20. Seibert CE, Dreisbach JN, Swanson WB, Edgar RE, Williams P, Hahn H. Progressive post-traumatic cystic myelopathy: neuroradiologic evaluation. *AJNR* **1981**;2:115–119
21. Kan S, Fox AJ, Vinuela F, Barnett HJM, Peerless SJ. Delayed CT metrizamide enhancement of syringomyelia secondary to tumor. *AJNR* **1983**;4:73–78
22. Quencer RM, Green BA, Eismont FJ. Posttraumatic spinal cord cysts: clinical features and characterization with metrizamide computed tomography. *Radiology* **1983**;146:415–423
23. Adams JH, Corsellis JAN, Duchen LW, eds. *Greenfield's neuropathology*, 4th ed. New York: Wiley Medical, **1984**:396–402
24. Sherman JL, Citrin CM, Gangarosa RE, Bowen BJ. The MR appearance of CSF pulsations in the spinal canal. *AJNR* **1986**;7:879–884
25. Rubenstein LJ. Tumors of the central nervous system. In *Atlas of tumor pathology*, 2nd series, fascicle 6. Washington, DC: Armed Forces Institute of Pathology, **1972**:10–12